

# Cybersecurity Entity Alignment via Masked Graph Attention Networks

Yue Qin

Indiana University Bloomington  
qinyue@iu.edu

Xiaojing Liao

Indiana University Bloomington  
xliao@indiana.edu

## Abstract

Cybersecurity vulnerability information is often recorded by multiple channels, including government vulnerability repositories, individual-maintained vulnerability-gathering platforms, or vulnerability-disclosure email lists and forums. Integrating vulnerability information from different channels enables comprehensive threat assessment and quick deployment to various security mechanisms. Efforts to automatically gather such information, however, are impeded by the limitations of today’s entity alignment techniques. In our study, we annotate the first cybersecurity-domain entity alignment dataset and reveal the unique characteristics of security entities. Based on these observations, we propose the first cybersecurity entity alignment model, CEAM, which equips GNN-based entity alignment with two mechanisms: *asymmetric masked aggregation* and *partitioned attention*. Experimental results on cybersecurity-domain entity alignment datasets demonstrate that CEAM significantly outperforms state-of-the-art entity alignment methods.

## 1 Introduction

There are many channels of cybersecurity vulnerability reports: Public vulnerability databases, including prominent U.S. government vulnerability repositories (e.g., the National Vulnerability Database), individual-maintained vulnerability-gathering platforms (e.g., Security Focus), vulnerability disclosure email lists and forums, and many others. Integrating such vulnerability information is essential for an organization to gain a big picture of the fast-evolving vulnerability landscape, timely identify early signs of cybersecurity risk, and effectively contain the threat with proper means. However, it is non-trivial to link the same vulnerabilities among different sources, as unique identifiers (e.g., CVE-ID) may not be mentioned in some repositories. The key step of cybersecurity information

integration is to link security entities (e.g., vulnerabilities) that refer to the same real-world entity across different data sources. This is an entity alignment (EA) problem on security Knowledge Graphs, which can be programmatically constructed from structured or semi-structured security reports. However, to the best of our knowledge, no previous study has investigated domain-specific entity alignment in the field of cybersecurity.

Traditional entity alignment methods based on hand-crafted rules are less successful since different KGs vary in structures and textual features (Zeng et al., 2021). More recent work (Hu et al., 2019) utilize Knowledge Graph Embedding (KGE) models trained towards triple plausibility (e.g., TransE (Bordes et al., 2013)) to align equivalent entities into a unified vector space based on a few seed alignments. However, such methods are not suitable for security entity alignment since the KGE models cannot generate embeddings for new entities added to the KG after training. The security information is always timely updated, and it is unrealistic to retrain the KG embedding model on the whole augmented graph each time new security entities (e.g., vulnerabilities) are revealed. (Mao et al., 2021) regards entity alignment as an assignment problem between two isomorphic graphs by reordering the entity node indices. However, it’s difficult to be adapted for security entity alignment because security KGs crafted from different repositories diverge in graph topology, and only a *subset* of entities on both KGs can be aligned. Inspired by the recent success of Graph Neural Network (GNN) on open-domain entity alignment (Wu et al., 2020; Mao et al., 2020; Nguyen et al., 2020), we propose a cybersecurity domain-specific entity alignment model to recognize the equivalent cyber-vulnerabilities. The GNN mechanism enables recursive information propagation among neighbors to learn structure-aware entity representations for the alignment. However, the core assumptions

that identical entities have similar attributes and neighbors and vice versa do not hold for cross-platform security entities. In our study, we observe identical vulnerability show inconsistent attributes (vulnerability artifacts, e.g, impact and affected version) in different vulnerability repositories (see Section 3.4). The main reason is that a vulnerability is sometimes assessed considering specific execution environments such as operating systems, architectures, configurations, and organization policies, which yields different vulnerability artifacts. In addition, different repositories provide vulnerability artifacts in different granularity (e.g., level of details), especially for the vulnerabilities disclosed in maillists and forums.

Therefore, in this paper, we propose the first cybersecurity-specific entity alignment model, CEAM. It equips GNN-based entity alignment model with two mechanisms: *asymmetric masked aggregation* and *partitioned attention*, to address the above challenges. We first aggregate *selective* attribute information to learn the semantic embeddings for security entities by an asymmetric mask. It propagates only a specific portion of attributes to the target entity, enforcing that the distance between two entities is narrowed down only when they are mutually the nearest candidate of each other. Further, we use GNNs to update entity embeddings with structural information based on graph topology, where the partitioned attention mechanism ensures that the artifacts critical to the vulnerability identification are always taken more consideration during the propagation. Finally, we use two-layer MLP (Mutilayer Perceptron) to decide whether two entities are identical according to the discrepancy between entity embeddings learned by GNNs. Our experiments show that the two mechanisms collectively improve alignment quality by 10.3% F1 score in average. Overall, the model achieves 81.5% F1 score. The contributions of this paper are as follows:

- We proposed the *first* cybersecurity-domain entity alignment model infused with domain knowledge towards cybersecurity information aggregation.
- We fixed the severe information loss (i.e., missing vulnerability identifiers) from the alignment results in even high-profile sources which deliver the most informative vulnerability presentation.
- We release the *first* annotated security KGs and cybersecurity-domain entity alignment datasets.

## 2 Background

### 2.1 Vulnerability profiling standard

According to CNA<sup>1</sup>, requesting identifiers for newly found vulnerabilities requires the information of vulnerability type, vendor, and the affected equipment. Additional information such as impact and discoverer is also encouraged. In our research, we regard these required and encouraged information as profiling artifacts. Other vulnerability artifacts like CVSS score, CVSS vector are considered as non-profiling artifacts.

### 2.2 GNN-based Entity Alignment

Most GNN-based entity alignment methods (Berrendorf et al., 2020; Zhu et al., 2020; Mao et al., 2020) are subject to the following framework: (1) a GNN to learn node representations from graph structure and (2) a margin-based loss to rank the distance between entity pairs. The loss function

$$L = \sum_{(i,j) \in \mathcal{P}} \sum_{(i',j') \in \mathcal{P}^-} \max \{d(h_i, h_j) - d(h_{i'}, h_{j'}) + \gamma, 0\}$$

aims at making equivalent entities  $(i, j)$  close to each other while maximizing the distance between negative pairs  $(i', j')$ . Here  $h_i$  is the embedding of entity  $i$  updated by a GNN layer in the form of:

$$h_i^{l+1} \leftarrow \sigma \left( \text{Aggregate} \left[ W^l \cdot h_k^l, \forall k \in (i \cup N_i) \right] \right)$$

where  $N_i$  is the set of neighboring nodes around node  $i$ ,  $W^l$  is the transformation matrix in layer  $l$ , and  $\sigma$  is a non-linear activation function. Instead of  $W^l$ , the relation-aware GNN learns a specific transformation matrix  $W_r^l$  for each relation  $r$ . GNN variants serve the purpose of *Aggregate* by different operations such as normalized mean pooling (Berrendorf et al., 2020) and weighted summation (Veličković et al., 2017). In this paper, we propose *masked aggregation* and *partitioned attention* in *Aggregate* operation to infuse security domain knowledge into the learning of entity embeddings.

## 3 Security Knowledge Graphs

In our study, we *first time* construct and release three annotated security KGs from one security information portal, i.e., SecurityFocus (SF) and two governmental repositories, i.e, National Vulnerability Database (NVD) and ICS-CERT Advisories (CERT). All reports are in English. The crawled data are for informational purposes only, following

<sup>1</sup> CVE Numbering Authorities: <https://cve.mitre.org/cve/cna.html>

Table 1: Common artifacts provided by security repositories. Profiling artifacts are in bold.

Source \ Artifact	CVE	CWE		CVSS v2&v3		CPE			Impact	Discoverer
		<b>weakness</b>	cwe-id	vector	score	<b>vendor</b>	<b>product</b>	affected version		
ICS-CERT	⊕	⊕	⊕	⊕	⊕	✓	✓	✓	✓	⊕
SF	✓	⊖				✓	✓	✓	✓	✓
NVD	✓	✓	✓	⊕	⊕	✓	✓	✓	✓	

† (✓: all reports, ⊕: large fraction of reports, ⊖: small fraction of reports).

all repositories’ terms of service. Across the three KGs, we build two EA datasets by linking entities from ICS-CERT and SecurityFocus to NVD. Below we explain the annotation process of the security KGs (Section 3.1, 3.2) and the EA dataset (Section 3.3). A quantitative study in Section 3.4 showing the particularity of the data demonstrates the challenges of aligning security entities.

### 3.1 KG schema

Figure 1 illustrates a general schema (i.e., entity types and relations) of the proposed security KGs. We design the KG schema by summarizing the common artifacts<sup>2</sup> provided by security reports, as shown in Table 7. These vulnerability artifacts can be interlinked by the concepts in the following standard security databases: Common Vulnerabilities and Exposures (CVE) for descriptions of publicly known vulnerabilities, Common Weakness Enumeration (CWE) for categorizing software security weaknesses, Common Platform Enumeration (CPE) for encoding names of IT products and platforms, and Common Vulnerability Scoring System (CVSS) for evaluating vulnerability severity.

### 3.2 KG Construction

For NVD, we construct the security KG by retrieving vulnerability information from an NVD database (Kiesling et al., 2019) and linking them according to our KG schema. For the other two semi-structured security repositories, we collected all available reports and annotated a subset of them. The annotation process are detailed as below.

**Gazeteer.** We build a vocabulary for vulnerability-related artifacts based on CPE and CWE to help us recognize mentions of security entities in text. In total, the dictionary contains 26,461 product names, 8,738 vendors, and 187,711 versions from CPE, and 1,029 weaknesses from CWE.

**Annotation Process.** The entities and relations of security KGs are annotated by three cybersecurity-

<sup>2</sup>Examples and explanations are shown in Appendix A.

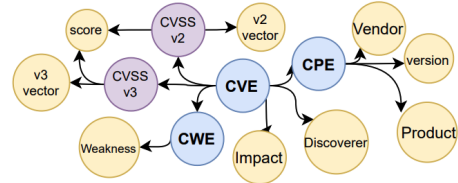


Figure 1: KG schema. Blue: entities; Yellow: literal artifacts; Purple: intermediate nodes.

Table 2: Annotation statistics. The agreement is measured with Fleiss’s kappa coefficient (Fleiss, 1971).

Repository	# Reports	# AnnotatedReports	Agreement
ICS-CERT	1,324	1,000	0.824
SecurityFocus	68,785	3,120	0.865

major students. The annotation standard is summarized through five preliminary rounds of annotation, covering 320 reports. In the first round, we discuss the context and the corresponding data entry of each vulnerability artifact in both repositories to summarize a set of patterns to extract entities and assign relations between them. In each following round, we resolve disagreements and refine the patterns. After the adjustment through five rounds, we programmatically parse all reports and manually verify a subset of them. The three annotators amend the annotation of each report in this subset, respectively, as shown in Table 2<sup>3</sup>. These annotations are merged into a final version by majority vote. The statistics of three security KGs are shown in Table 3. The data is released with the consent from all annotators.

<sup>3</sup>To calculate Fleiss’s kappa, we take triples recognized by three annotators as samples, and the types of triples (including *NotRecognized*) as categories.

Table 3: Statistics of security KGs. #Ntypes represents the number of node types.

Security KG	# Nodes	# Edges	# NTypes	# Relations
NVD	24,069	82,338	11	13
ICS-CERT	4,700	21,996	12	14
SecurityFocus	7,011	23,712	7	8

Table 4: Statistics of KGs for Alignment.

Dataset	#AlignedEnt	#SharedArt	#TotalArt
CERT-NVD	987	514	19,721
SF-NVD	1,607	1,303	20,000

### 3.3 Annotation of Alignment Data

We build two alignment datasets using the same data format with (Zhu et al., 2020), which consists of two KGs along with positive and negative entity pairs. We consider NVD knowledge graph as the target KG and align the two other KGs to it, for NVD is the standard database with the highest coverage of vulnerabilities. Each alignment dataset includes vulnerability artifacts that are *jointly* presented by both two KGs, except for the vulnerability identifiers, i.e., CVE-ID. Records with two and above missing artifacts are dropped in this process. Finally, we have 7,368, 1,136, and 2,410 vulnerabilities in KGs of NVD, ICS-CERT, and SecurityFocus for security entity alignment.

We label the identical entities in different sources based on the same reference of common identifiers (e.g., CVE-ID, CWE-ID, CPE serial number) and security checklist references (i.e., hyperlinks of the same vulnerability to the other repositories) in the NVD database. Table 4 shows the statistics of KGs to be aligned, including the number of co-occurred vulnerabilities and artifacts across two KGs and the total number of artifacts. For negative alignments, we randomly sample 10 negative entities from the other KG for each entity in all positive pairs. We also sample 10 negative pairs for entities on the source KG without a corresponding alignment on the target KG. In total, the alignment dataset contains 2,594 positive pairs and 65,710 negative pairs.

### 3.4 Findings

In the security KGs, we observe the attribute inconsistency between positive entity pairs and attribute similarity between negative entity pairs, compared with entity alignment datasets in other domains. We elaborate our findings as below.

**Inconsistencies in positive pairs.** We denote that a pair of entities encounter an attribute inconsistency in a certain type if no match exists between their attributes in this type. Here, a match means the tokens are the same, or one token is a substring of another. Among all the positive pairs in our dataset, 56.0% pairs of vulnerabilities have attribute inconsistency in more than half of attribute

types. However, in the entity alignment datasets of music and movie (Zhu et al., 2020), only 8.3% positive entity pairs face the same problem. The attribute inconsistencies hinder the classifier from making correct positive decisions. To alleviate this problem, we propose a masked gate to aggregate neighboring attributes selectively.

**Similarity in negative pairs.** We observe that different vulnerabilities can be associated with quite many identical artifacts. More specifically, among all negative pairs in our alignment datasets, 4.04% differ in only one quarter types of artifacts. As a comparison, with the same negative sampling ratio, only 1.14% negative pairs in the music dataset in (Zhu et al., 2020) have the same problem. Such circumstances make it difficult for the classifier to distinguish different-but-similar entities. Based on the vulnerability profiling standard and our observation on the datasets, to distinguish a vulnerability from a set of known vulnerabilities, at least one of its *profiling* artifacts should be different. Therefore, higher attention on the profiling artifacts helps preserve the distinction between similar entities. Accordingly, we propose a partitioned attention mechanism to assign higher importance weights to the profiling artifacts in a mandatory way.

## 4 Problem Formulation

We represent the security knowledge graph as a heterogeneous graph  $G$  connecting nodes in types  $\mathcal{A}$  by relations  $\mathcal{R}$ . We use a set of nodes  $\mathcal{V}$  to denote security entities with a mapping  $\psi : \mathcal{V} \rightarrow \mathcal{A}$  to the entity types. The security KG is modeled as a set of triples  $G(\mathcal{V}, \mathcal{A}, \mathcal{R}) = \{t | t : (i, r, j), i, j \in \mathcal{V}, r \in \mathcal{R}\}$ . Entity types and relations are aligned in advance: for a certain  $G^*$ , its entity types  $\mathcal{A}^*$  and relations  $\mathcal{R}^*$  are aligned to the KG schema in Section 3.1 during KG construction.

**Security entity alignment.** Given a source knowledge graph  $G(\mathcal{V}, \mathcal{A}, \mathcal{R})$  and a target knowledge graph  $G'(\mathcal{V}', \mathcal{A}', \mathcal{R}')$ , entity alignment aims at finding the identical target entity  $v' \in \mathcal{V}'$  for each source entity  $v \in \mathcal{V}$ . However, in the security domain, only a few entities on one KG has the same real-world reference on another. Therefore, we define the security entity alignment problem as follows: Given a set of entity pairs  $S = \{(v_s, v'_s) \in \mathcal{V}_s \times \mathcal{V}'_s, \mathcal{V}_s \subset \mathcal{V}, \mathcal{V}'_s \subset \mathcal{V}'\}$  between two knowledge graphs  $G$  and  $G'$ , security entity alignment aims to determine whether each entity pair in  $\{(v_i, v'_i) \in (\mathcal{V} \times \mathcal{V}') \setminus S\}$  refer to the same real word objects with high precision and recall.

## 5 Method

CEAM applies a joint GNN framework to address the security entity alignment problem. CEAM consists of an aggregate layer that initializes entity representation by masked neighborhood information, a 2-layer GNN that embeds structural information in node representation, and a classifier that makes the alignment decision according to node distance. As in (Zhu et al., 2020), we model the security entity alignment as a binary classification problem on a given set of positive and negative entity pairs. The entire model is jointly trained by the cross entropy loss:  $L = -\frac{1}{N} \sum_i [y_i \log p_i + (1 - y_i) \log(1 - p_i)]$ , where  $y_i$  labels whether the two entities in pair  $i$  refer to the same object. Below we describe the two proposed mechanisms that enhance the GNN to learn better embeddings for security entities.

### 5.1 Masked Attribute Aggregation

We use masked attribute aggregation to represent ID-like entities from neighborhood literal artifacts. Due to the heterogeneity of knowledge graphs, we first aggregate the representation of artifacts in the same type into relation representation. Further, we use the similarity between the relations representation of different entities to calculate the mask, an attribute-level scaling operator for aggregating relation representation into entity representation. The mask relaxes the similarity constraint of a candidate pair of entities if they are mutually the most closed ones over the two KGs. Below we elaborate on the two-stage masked aggregation.

**Stage 1: towards relation representation.** For node  $i$  on the graph  $G(\mathcal{V}, \mathcal{A}, \mathcal{R})$ , its corresponding relation  $r$  is represented as

$$\phi_i(r) = \sum_{j \in N_{i,r}} \alpha_{irj} W_r h_j,$$

where  $W_r$  is the transform weight for relation  $r$ ,  $N_{i,r} = \{j | (i, r, j) \in G\}$  represents the neighbors associated with  $i$  by relation  $r$ ,  $\alpha_{irj}$  characterizing the importance of node  $j$  to node  $i$  is the relative co-occurrence rate of two nodes across two KGs:

$$\alpha_{irj} = \frac{\exp(-d_j(d_j + d'_j)^{-1})}{\sum_{k \in N_{i,r}} \exp(-d_k(d_k + d'_k)^{-1})},$$

where  $d_j$  and  $d'_j$  are the number of entities connected to node  $j$  on graph  $G$  and  $G'$ , respectively. Such design follows two considerations: 1) the neighbors connected with fewer entities on the source side are more specific and representative to the entity, and 2) the neighbors that are jointly linked with the positive entity pairs will benefit the

alignment. For example, NVD provides both devices and configures (e.g., software, hardware, etc.) as the affected products of a cyber vulnerability, while most reports in CERT mainly contain device information. Therefore, it is more likely to boost a positive align if the attributes of the device are emphasized to represent the relation `affected products`. Also, some basic architectures in cyber systems, like SCADA (Supervisory Control And Data Acquisition System), which frequently appear in various security reports, are less representative to profile a specific vulnerability or distinguish different vulnerabilities.

**Stage 2: towards entity representation.** By stacking the relation representation  $\phi_i(r)$ , entity  $i$  is temporarily encoded by the matrix:  $\Phi_i = (\phi_i(r_1)^T, \phi_i(r_2)^T, \dots, \phi_i(r|\mathcal{R})^T)$ . Further, we study a mask gate that scales the attributes (i.e., features) of the relation representation during the aggregation. To do this, we consider a scaling parameter  $m$  for each attribute  $t$  in the representation of  $r$ , which reflects the confidence that entity  $i$  possesses the attribute. We construct a set of candidates  $\mathcal{C}_i = \{i' | \exists j \in (\mathcal{V} \cap \mathcal{V}') : (i, r, j) \in \mathcal{G} \wedge (i', r, j) \in \mathcal{G}'\}$  for entity  $i$ . The scaling parameter  $m_{i,r}^t$  is measured by the consistency of the attribute  $t$  in the representation of  $r$  among all candidate pairs  $\{(i, i')\}$  of  $i$ ,

$$m_{i,r}^t = \exp\left(-\sum_{i' \in \mathcal{C}_i} c_{ii'} [\phi_i^t(r) - \phi_{i'}^t(r)]^2\right),$$

where  $\phi_i^t(r)$  is the value of attribute,  $c_{ii'} = \text{softmax}_{i' \in \mathcal{C}_i} (-\|\Phi_i - \Phi_{i'}\|_F)$  indicates the correspondence of  $i'$  to  $i$ . Therefore, for the complete relation representation  $\phi_i(r)$ , we can define the mask gate altogether as a *diagonal* matrix  $M_i^r$ ,

$$M_i^r = \exp\left(-\sum_{i'} c_{ii'} \cdot \mathbf{d}_r(i, i') \mathbf{d}_r(i, i')^T\right),$$

where  $\mathbf{d}_r(i, i') = \phi_i(r) - \phi_{i'}(r)$ . Finally we have the aggregated representation of entity  $i$  as:

$$h_i = \frac{1}{|\mathcal{R}|} \sum_r M_i^r \phi_i(r)$$

The mask reduces the effect of different attributes between a candidate pair of entities only if they are *mutually* the most closed ones to each other among two KGs; Otherwise, the distance between the masked entity representations will not decrease since the masks are asymmetric and scale different attributes for the two entities. This enables CEAM to achieve high recall while preserving tolerable precision for security entity alignment.

## 5.2 GNN with Partitioned Attention

In GNN encoder, we learn transformations  $W_t$  for each entity type and  $W_r$  for each relation. As in (Zhu et al., 2020), we calculate node-level attention  $s$  and relation-level attention  $\beta$  to accumulate neighborhood information:

$$z_i = \sum_{r,j \in N_{i,r}} s_{irj} \cdot \beta_{ir} \cdot W_r h_j,$$

and combines the self information  $h_i^{(l-1)}$  and accumulated neighborhood information  $z_i$ :

$$h_i^{(l)} = \sigma \left( [W_t^{(l)} \cdot h_i^{(l-1)} || z_i] \right).$$

The node-level attention  $s_{irj}$  is defined as the cosine similarity between two connected nodes:

$$s_{irj} = \text{cos\_sim} \langle W_t^{(l)} h_i^{(l-1)}, W_r^{(l)} h_j^{(l-1)} \rangle,$$

and the relation-level attention  $\beta_{ir}$  is collectively decided by whether the relation is predefined as critical and the similarity between nodes. We consider the profiling relations  $R_P$  as the set of relations connecting profiling artifacts (See Section 2.1) with entities. Let the profiling ratio  $\rho = \frac{|R_P|}{|R|}$ . Accordingly, we define the partisan term  $\delta$  with a positive hyper-parameter  $\epsilon$  where  $0 < \epsilon < 1 - \rho$ :

$$\delta_{R_X} = \begin{cases} \rho + \epsilon - 0.5 & \text{if } R_X = R_P \\ -\rho - \epsilon + 0.5 & \text{if } R_X = R \setminus R_P \end{cases},$$

where  $R_X$  represents the group of profiling or non-profiling relations. And the attention weight for  $r \in R_X$  is

$$\beta_{ir} = \left( \frac{1}{2} + \delta_{R_X} \right) \underset{r \in R_X}{\text{softmax}} \left( |N_{i,r}|^{-1} \sum_{j \in N_{i,r}} s_{irj} \right),$$

Such a mechanism ensures that critical relations (e.g., affected products, etc.) suggested by vulnerability profiling standards are emphasized while reserving the relative importance within a relation group (i.e., profiling or non-profiling).

## 6 Experiments

### 6.1 Experimental Settings

**Dataset and data processing.** We set the train-test-split rate as 0.25, and use a 5-fold cross validation on the training set to select hyperparameters, e.g., the learning rate. For the alignment targets, i.e., vulnerability entities, we replace the original CVE-IDs with randomly assigned numerical IDs so entities in a positive pair are represented

by different tokens. Other artifact entities are initialized with textual representations. We train a Word2Vec (Church, 2017) model using Gensim (Rehrek et al., 2011) with all available reports, and use fastText (Joulin et al., 2016) to encode textual features of artifact entities as 100-dimensional vectors for all of the GNN-based methods.

**Evaluation metrics.** We apply three metrics: Precision@Recall=0.95, F1, and PRAUC (precision-recall area under curve). For the first metric, we tune the alignment threshold during testing and report the highest precision when the recall reaches the given value. A higher recall value is more desirable in the security applications (Yang et al., 2021) to recover the identities of vulnerabilities missing identifiers, where the false positives can be excluded through handful manual verification. For F1 evaluation we use the decision threshold that achieves the highest macro F1 during validation.

**Hyperparameters.** For each model, we apply a binary search from 0.001 to 0.1 on the validation set for learning rate selection. The best learning rate for CERT-NVD dataset and SF-NVD dataset are 0.02 and 0.025, respectively. The dimension of GNN embeddings in CEAM and baselines is 64.

**Computation Cost.** The complexity of CEAM is  $O(|V| \cdot (N + C) \cdot \frac{S}{B})$ , where  $N$  is the maximum neighborhood size,  $C$  is the maximum candidate size,  $S$  is the training size and  $B$  is the batch size. The model has 340,309 parameters. We run CEAM on Intel Core i5-3550 3.30GHz 4-Core Processor with NVIDIA GTX 1070 Ti GPU. Averagely, each batch of size 128 costs 295.3 ms for training.

### 6.2 Baselines

**EA w/o. one-to-one constraint.** We compare the proposed method with the following state-of-the-art methods: *CG-MuAlign* (Zhu et al., 2020) features a collective GNN framework to align entities in two domains: music and movie. It also formalizes the alignment problem as a classification task on a given set of entity pairs. *PARIS* (Suchanek et al., 2011) is a conventional method that align entities by probabilistic reasoning. Several studies (Mao et al., 2021; Zhao et al., 2020) have noted that *PARIS* outperforms many ‘‘advanced’’ EA models. *PRASE* (Qi et al., 2021) is an extension of *PARIS*, which incorporates the translation-based EA models to boost the alignment decisions.

**GNN variants.** We evaluate the recent GNN models in security entity alignment, as shown in Table 5. R-GCN, R-GAT, and R-GraphSage are the vari-

Table 5: Results of Cybersecurity Entity Alignment.

Method	CERT-NVD			SF-NVD		
	Pre@Rec=.95	F1	PRAUC	Pre@Rec=.95	F1	PRAUC
GCN	0.198 ± .002	0.330 ± .004	0.265 ± .006	0.139 ± .004	0.233 ± .003	0.172 ± .002
GAT	0.201 ± .005	0.340 ± .008	0.357 ± .003	0.165 ± .002	0.274 ± .001	0.293 ± .002
GraphSage	0.179 ± .001	0.327 ± .003	0.303 ± .004	0.128 ± .005	0.216 ± .003	0.207 ± .001
R-GCN	0.361 ± .003	0.475 ± .003	0.421 ± .005	0.267 ± .002	0.456 ± .003	0.412 ± .002
R-GAT	0.392 ± .004	0.610 ± .002	0.654 ± .003	0.293 ± .004	0.541 ± .006	0.562 ± .004
R-GraphSage	0.290 ± .002	0.450 ± .005	0.413 ± .009	0.199 ± .005	0.414 ± .018	0.382 ± .010
PARIS	--	0.712 ± .000	0.543 ± .000	--	0.611 ± .000	0.346 ± .000
PRASE(BootEA)	--	0.731 ± .000	0.576 ± .000	--	0.620 ± .000	0.477 ± .000
PRASE(MultiKE)	--	0.706 ± .000	0.512 ± .000	--	0.609 ± .000	0.398 ± .000
CGMuAlign	0.470 ± .026	0.761 ± .012	0.720 ± .003	0.328 ± .013	0.654 ± .021	0.576 ± .007
CEAM	0.778 ± .015	0.843 ± .015	0.875 ± .002	0.694 ± .011	0.787 ± .021	0.801 ± .004

ants of GCN, GAT, and GraphSage which train specific transformation weights for each relation. We reimplement all of the GNN variants with DGL (Wang et al., 2019). CEAM and all the GNN variants use the same model structures: 2-layer GNNs following with two fully-connected layers.

We use the EA datasets in Section 3.3 to evaluate CEAM, CGMuAlign, and all GNN variants. For PARIS and PRASE, we generate datasets with the format in (Qi et al., 2021). To ensure the comparability, for the results of PARIS and PRASE, we only consider the wrong alignments sampled in our negative pairs (See Section 3.3) as false positives.

### 6.3 Effectiveness

Table 5 shows the averaged alignment results of three runs on the two datasets. All models show higher performance on CERT-NVD dataset than SF-NVD dataset. The main reason is that SF knowledge graphs provide fewer entity types and suffer more from sparsity issues. Overall, CEAM outperforms all other methods. CG-MuAlign, which is similar in problem formulation and model architecture with CEAM, shows the second best result. PARIS is less successful to identify the same entities in security KGs. Compared with PARIS, PRASE improves 1.9% on averaged F1 by incorporating translation-based alignment modules. Note that CEAM has significantly better performance on Pre@Rec=0.95. This is mainly because the proposed mechanisms enable CEAM to achieve high recall even with a rather large decision threshold. In contrast, previous EA models attach less importance to preventing false negatives and the decision threshold needs to be very small to achieve high recall, which greatly reduces the precision. More specifically, CEAM employs masked aggregation to relax the similarity constraints for positive aligns, which

Table 6: Analysis of proposed method.

Method	P@R=0.95	F1
<b>w.o.</b> masked aggregation	0.516	0.712
<b>w.o.</b> mask (=mean aggregate)	0.532	0.763
<b>w.o.</b> partitioned attention	0.687	0.790
<b>w.o.</b> non-profiling artifacts	0.665	0.775
CEAM	0.736	0.815

decreases false negatives to achieve high recall. In the meantime, such relaxation is only applied when the two entities are mutually the most closed candidate to each other, which preserves evidence for negative aligns to prevent low precision.

### 6.4 Ablation Study

Table 6 shows the improvement by each proposed mechanism, respectively. All the scores are averaged on the two alignment datasets. The variant without both two mechanisms is equivalent to the baseline model using R-GAT to train node representations. Overall, CEAM outperforms baselines by 23% F1 score. Below we detail the quantitative improvement by the two proposed mechanisms.

**Masked aggregation.** The first row of Table 6 shows the model effectiveness without any aggregation. The second row shows the result where the vulnerability entity representations are initialized as the mean of its neighboring artifacts. The results show that the aggregation operation boost the performance by 5.1% in averaged F1, and the mask mechanism further improves 5.2% averaged F1.

**Partitioned attention.** We present the alignment result using traditional attention mechanism where  $\alpha_{irj} = \text{softmax}_{r \in R, j \in N_{i,r}} \sigma(\bar{w}_r^T [h_i | W_r h_j])$  and  $z_i = \sum_{r \in R} \sum_{j \in N_{i,r}} \alpha_{irj} W_r h_j$  in the third and fourth row of Table 6. Compared with traditional attention operation on all entity types, the partition mecha-

nism enhances 2.5% averaged F1, since the profiling artifacts are enforced to be emphasized to alleviate the noises introduced by non-profiling artifacts. We also compare the result on dataset that only employs profiling artifacts while dropping the non-profiling ones. The result shows that the non-profiling artifacts still provide useful information to improve 1.5% F1. We evaluate the performance varying the hyper-parameter  $\epsilon$  (See Section 5.2) and the result is shown in Figure 2 in Appendix B.

## 7 Discussion

**Findings.** Among the 3,546 annotated vulnerabilities, 52 are released in reports without the identifier. Such vulnerability entities do not appear in the entity alignment datasets since their corresponding NVD vulnerabilities are unknown. We construct the candidate pairs for such vulnerabilities as described in Section 5.1 and run CEAM to predict their binary labels. Finally, we manually verify the *positive* alignments according to the reference checklist and the artifacts provided from both sides, and find 70.2% of them are correct, which recovers the missing vulnerability identifiers for 28 reports.

**Limitations.** Our research demonstrates that the proposed domain-driven mechanisms benefit security entity alignment. Most false positives are produced in vulnerabilities with similar impacts and the same other artifacts. The representations of such underlying different vulnerabilities are very closed, and it’s hard to distinguish them for all similarity-based alignment methods. Meanwhile, the false negatives are mainly due to data quality issues such as information inconsistency, which is commonly observed in real-world vulnerability repositories (Dong et al., 2019; Anwar et al., 2021; Jiang et al., 2021). For example, the affected product, vendor, and weakness of CVE-2018-7084 provided by ICS-CERT and NVD are all different. Although the mask mechanism relaxes the similarity constraint, CEAM cannot align the two records in this case. We leave the entity alignment with information quality assessment as future work.

## 8 Related Works

**Graph Entity Alignment.** Recent graph entity alignment methods assume that same entities on different KGs have: (1) similar attribute distributions, and (2) similar neighborhood structures. Accordingly, translation-based methods (Hao et al., 2016; Chen et al., 2016; Zhu et al., 2017; Sun et al., 2017, 2018; Hu et al., 2019) use knowledge graph embed-

ding models to generate entity embeddings from triple structures; GNN-based methods (Berrendorf et al., 2020; Wu et al., 2019; Cao et al., 2019; Wu et al., 2020; Nguyen et al., 2020; Mao et al., 2020; Zhu et al., 2021) apply graph convolution operations to utilize neighborhood information. Further, (Pei et al., 2020) proposes reinforced training strategy to achieve noise-aware entity alignment; (Yan et al., 2021) proposes topology-invariant gates to dynamically align evolving knowledge graphs. By applying graph isomorphism, (Mao et al., 2021) learns a permutation matrix that transforms one KG to another by reordering the entity node indices.

**Domain-specific entity linking.** To disambiguate candidate entities for the given mentions, (Inan and Dikenelli, 2018) utilizes domain information to filter candidates; (Shen et al., 2018) designs a probabilistic linking model that combines the distribution of entities and domains; (Klie et al., 2020) proposes entity linking for low-source domains by letting human annotators make corrections on ranked candidate entities for each mention. All existing works utilize domain information to constrain the search space of candidates, while the domain-specific properties are overlooked.

**Security entity identification.** Cross-platform entity identification has been studied in the security domain to combat the evolving cybercrimes. (Xu et al., 2017) detects the similarity of cross-platform binary code functions based on a graph embedding generation network. (Zhang et al., 2019) and (Fan et al., 2019) build weighted multi-view networks based on user relatedness and apply GCN for node representations to identify key players in cybercriminal communities or link cross-platform suspicious accounts. To the best of our knowledge, we are the first to incorporate the properties of security entities into the alignment process.

## 9 Conclusion

In this paper, we construct the first annotated cybersecurity-domain entity alignment datasets and reveal the attribute inconsistency feature of security entities. Based on this feature, we propose the first cybersecurity entity alignment model, CEAM, which equips GNN-based entity alignment model with two mechanisms, asymmetric masked aggregation and partitioned attention. Experimental results on cybersecurity-domain entity alignment datasets demonstrate the effectiveness of our method, which outperforms the state-of-the-art.



## References

- Afsah Anwar, Ahmed Abusnaina, Songqing Chen, Frank Li, and David Mohaisen. 2021. Cleaning the nvd: Comprehensive quality assessment, improvements, and analyses. *IEEE Transactions on Dependable and Secure Computing*.
- Max Berrendorf, Evgeniy Faerman, Valentyn Melnychuk, Volker Tresp, and Thomas Seidl. 2020. Knowledge graph entity alignment with graph convolutional networks: Lessons learned. *Advances in Information Retrieval*, 12036:3.
- Antoine Bordes, Nicolas Usunier, Alberto Garcia-Duran, Jason Weston, and Oksana Yakhnenko. 2013. Translating embeddings for modeling multi-relational data. *Advances in neural information processing systems*, 26.
- Yixin Cao, Zhiyuan Liu, Chengjiang Li, Juanzi Li, and Tat-Seng Chua. 2019. Multi-channel graph neural network for entity alignment. *arXiv preprint arXiv:1908.09898*.
- Muhao Chen, Yingtao Tian, Mohan Yang, and Carlo Zaniolo. 2016. Multilingual knowledge graph embeddings for cross-lingual knowledge alignment. *arXiv preprint arXiv:1611.03954*.
- Kenneth Ward Church. 2017. Word2vec. *Natural Language Engineering*, 23(1):155–162.
- Ying Dong, Wenbo Guo, Yueqi Chen, Xinyu Xing, Yuqing Zhang, and Gang Wang. 2019. Towards the detection of inconsistencies in public security vulnerability reports. In *28th {USENIX} Security Symposium ({USENIX} Security 19)*, pages 869–885.
- Yujie Fan, Yiming Zhang, Shifu Hou, Lingwei Chen, Yanfang Ye, Chuan Shi, Liang Zhao, and Shouhuai Xu. 2019. idev: Enhancing social coding security by cross-platform user identification between github and stack overflow. In *28th International Joint Conference on Artificial Intelligence (IJCAI), 2019*.
- Joseph L Fleiss. 1971. Measuring nominal scale agreement among many raters. *Psychological bulletin*, 76(5):378.
- Yanchao Hao, Yuanzhe Zhang, Shizhu He, Kang Liu, and Jun Zhao. 2016. A joint embedding method for entity alignment of knowledge bases. In *China Conference on Knowledge Graph and Semantic Computing*, pages 3–14. Springer.
- Wei Hu, Qingheng Zhang, Zequn Sun, and Jiacheng Huang. 2019. Multike: a multi-view knowledge graph embedding framework for entity alignment. In *OM@ ISWC*, pages 189–190.
- Emrah Inan and Oguz Dikenelli. 2018. [A sequence learning method for domain-specific entity linking](#). In *Proceedings of the Seventh Named Entities Workshop, NEWS@ACL 2018, Melbourne, Australia, July 20, 2018*, pages 14–21. Association for Computational Linguistics.
- Yuning Jiang, Manfred Jeusfeld, and Jianguo Ding. 2021. Evaluating the data inconsistency of open-source vulnerability repositories. In *The 16th International Conference on Availability, Reliability and Security*, pages 1–10.
- Armand Joulin, Edouard Grave, Piotr Bojanowski, Matthijs Douze, H erve J egou, and Tomas Mikolov. 2016. Fasttext. zip: Compressing text classification models. *arXiv preprint arXiv:1612.03651*.
- Elmar Kiesling, Andreas Ekelhart, Kabul Kurniawan, and Fajar Ekaputra. 2019. The sepses knowledge graph: An integrated resource for cybersecurity. In *The Semantic Web – ISWC 2019*, pages 198–214. Cham. Springer International Publishing.
- Jan-Christoph Klie, Richard Eckart de Castilho, and Iryna Gurevych. 2020. [From zero to hero: Human-in-the-loop entity linking in low resource domains](#). In *Proceedings of the 58th Annual Meeting of the Association for Computational Linguistics, ACL 2020, Online, July 5-10, 2020*, pages 6982–6993. Association for Computational Linguistics.
- Xin Mao, Wenting Wang, Yuanbin Wu, and Man Lan. 2021. From alignment to assignment: Frustratingly simple unsupervised entity alignment. *arXiv preprint arXiv:2109.02363*.
- Xin Mao, Wenting Wang, Huimin Xu, Yuanbin Wu, and Man Lan. 2020. Relational reflection entity alignment. In *Proceedings of the 29th ACM International Conference on Information & Knowledge Management*, pages 1095–1104.
- Tam Thanh Nguyen, Thanh Trung Huynh, Hongzhi Yin, Vinh Van Tong, Darnbi Sakong, Bolong Zheng, and Quoc Viet Hung Nguyen. 2020. Entity alignment for knowledge graphs with multi-order convolutional networks. *IEEE Transactions on Knowledge and Data Engineering*.
- Shichao Pei, Lu Yu, Guoxian Yu, and Xiangliang Zhang. 2020. Rea: Robust cross-lingual entity alignment between knowledge graphs. In *Proceedings of the 26th ACM SIGKDD International Conference on Knowledge Discovery & Data Mining*, pages 2175–2184.
- Zhiyuan Qi, Ziheng Zhang, Jiaoyan Chen, Xi Chen, Yuejia Xiang, Ningyu Zhang, and Yefeng Zheng. 2021. [Unsupervised knowledge graph alignment by probabilistic reasoning and semantic embedding](#). In *Proceedings of the Thirtieth International Joint Conference on Artificial Intelligence, IJCAI 2021, Virtual Event / Montreal, Canada, 19-27 August 2021*, pages 2019–2025. ijcai.org.
- Radim Rehrek, Petr Sojka, et al. 2011. Gensim—statistical semantics in python. *Retrieved from gensim.org*.
- Wei Shen, Jiawei Han, Jianyong Wang, Xiaojie Yuan, and Zhenglu Yang. 2018. [SHINE+: A general framework for domain-specific entity linking with](#)

- heterogeneous information networks. *IEEE Trans. Knowl. Data Eng.*, 30(2):353–366.
- Fabian M. Suchanek, Serge Abiteboul, and Pierre Senellart. 2011. **PARIS: probabilistic alignment of relations, instances, and schema**. *Proc. VLDB Endow.*, 5(3):157–168.
- Zequn Sun, Wei Hu, and Chengkai Li. 2017. Cross-lingual entity alignment via joint attribute-preserving embedding. In *International Semantic Web Conference*, pages 628–644. Springer.
- Zequn Sun, Wei Hu, Qingheng Zhang, and Yuzhong Qu. 2018. Bootstrapping entity alignment with knowledge graph embedding. In *IJCAI*, volume 18, pages 4396–4402.
- Petar Veličković, Guillem Cucurull, Arantxa Casanova, Adriana Romero, Pietro Lio, and Yoshua Bengio. 2017. Graph attention networks. *arXiv preprint arXiv:1710.10903*.
- Minjie Wang, Da Zheng, Zihao Ye, Quan Gan, Mufei Li, Xiang Song, Jinjing Zhou, Chao Ma, Lingfan Yu, Yu Gai, Tianjun Xiao, Tong He, George Karypis, Jinyang Li, and Zheng Zhang. 2019. Deep graph library: A graph-centric, highly-performant package for graph neural networks. *arXiv preprint arXiv:1909.01315*.
- Yuting Wu, Xiao Liu, Yansong Feng, Zheng Wang, and Dongyan Zhao. 2019. Jointly learning entity and relation representations for entity alignment. *arXiv preprint arXiv:1909.09317*.
- Yuting Wu, Xiao Liu, Yansong Feng, Zheng Wang, and Dongyan Zhao. 2020. Neighborhood matching network for entity alignment. *arXiv preprint arXiv:2005.05607*.
- Xiaojun Xu, Chang Liu, Qian Feng, Heng Yin, Le Song, and Dawn Song. 2017. Neural network-based graph embedding for cross-platform binary code similarity detection. In *Proceedings of the 2017 ACM SIGSAC Conference on Computer and Communications Security*, pages 363–376.
- Yuchen Yan, Lihui Liu, Yikun Ban, Baoyu Jing, and Hanghang Tong. 2021. Dynamic knowledge graph alignment. In *Proceedings of the AAAI Conference on Artificial Intelligence*, volume 35, pages 4564–4572.
- Guanqun Yang, Shay Dineen, Zhipeng Lin, and Xueqing Liu. 2021. Few-sample named entity recognition for security vulnerability reports by fine-tuning pre-trained language models. In *Deployable Machine Learning for Security Defense. MLHat 2021. Communications in Computer and Information Science*, volume 1482, pages 55–78, Cham. Springer.
- Kaisheng Zeng, Chengjiang Li, Lei Hou, Juanzi Li, and Ling Feng. 2021. A comprehensive survey of entity alignment for knowledge graphs. *AI Open*, 2:1–13.
- Yiming Zhang, Yujie Fan, Yanfang Ye, Liang Zhao, and Chuan Shi. 2019. Key player identification in underground forums over attributed heterogeneous information network embedding framework. In *Proceedings of the 28th ACM international conference on information and knowledge management*, pages 549–558.
- Xiang Zhao, Weixin Zeng, Jiuyang Tang, Wei Wang, and Fabian Suchanek. 2020. An experimental study of state-of-the-art entity alignment approaches. *IEEE Transactions on Knowledge & Data Engineering*, (01):1–1.
- Hao Zhu, Ruobing Xie, Zhiyuan Liu, and Maosong Sun. 2017. Iterative entity alignment via knowledge embeddings. In *Proceedings of the International Joint Conference on Artificial Intelligence (IJCAI)*.
- Qi Zhu, Hao Wei, Bunyamin Sisman, Da Zheng, Christos Faloutsos, Xin Luna Dong, and Jiawei Han. 2020. **Collective multi-type entity alignment between knowledge graphs**. In *Proceedings of The Web Conference 2020*.
- Renbo Zhu, Meng Ma, and Ping Wang. 2021. Raga: Relation-aware graph attention networks for global entity alignment. In *Pacific-Asia Conference on Knowledge Discovery and Data Mining*, pages 501–513. Springer.

## A Entities and Relations

We present concrete examples of vulnerability artifacts in Table 7 and the explanations as below. *CVE* is the common identifiers of cybersecurity vulnerabilities. *Weakness* characterizes the category of the vulnerability, and *CWE\_ID* is the identifier of Weakness. *Product* and *Vendor* are the name and the provider of the affected products (e.g., software, hardware, device, etc). *Version* is short for affected versions. *Impact* is the consequence of exploiting the vulnerability. *Discoverer* is the name of the person or the organization who reported the vulnerability. In a triplet  $(h, r, t)$ , the relation  $r$  is decided by the types of the head entity  $h$  and the tail entity  $t$  and is in the form of *hasTail*. For example, the relation between a *Vulnerability* entity and a *Discoverer* is *hasDiscoverer*.

## B Hyper-parameter Analysis

We evaluate the performance varying the partisan term decided by  $\epsilon$  in Section 5.2 and the results are shown in Figure 2. The profiling ratio  $\rho$  (i.e., the portion of profiling relations among all relations) of the two alignment datasets (i.e., CERT-NVD and SF-NVD) are 0.4 and 0.8, respectively.

Table 7: Examples of vulnerability artifacts.

Artifact	Example
CVE	CVE-2019-34623
CWE_ID	CWE-200
Weakness	Information Exposure
Vendor	Siemens
Product	SINEMA Remote Connect Server
version	2.0 SP1
Impact	denial of service
Discoverer	Hendrik Derre, Tijl Deneut
CVSSv3 vector	AV:N/AC:L/PR:L/UI:N/S:U/C:L/I:N/A:N
CVSSv2 vector	AV:N/AC:L/Au:S/C:P/I:N/A:N
CVSSv3 score	V3 4.3
CVSSv2 score	V2 4.0

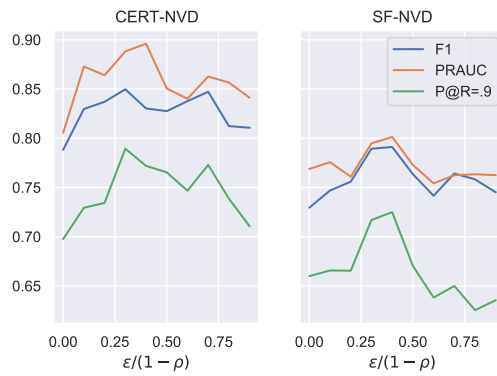


Figure 2: Model performance with different partisan term. X-axis shows the ratio between  $\epsilon$  and  $1 - \rho$ .